

Strikers with different nose shape impacting an armour steel - numerical modelling

Teresa Fras¹, Norbert Faderl¹, Christian C. Roth², D. Mohr²

¹French-German Research Institute of Saint-Louis (ISL), Saint-Louis, France

²Department of Mechanical and Process Engineering, ETH Zurich, Switzerland

The presented experimental investigation concerns 3 mm thick target plates impacted by strikers with different noses at velocity close to 300 m/s and is conducted to gain an insight into mechanisms of deformation and fracture characteristic for a high strength high hardness armour steel, [1]. Guaranteed by the producer yield strength and ultimate tensile strength of the steel are 1300 MPa and 2200 MPa, and the hardness is within 600 – 640 HB, [2]. Due to impacts, the projectiles and targets, both extracted from the armour steel, are severely deformed and fractured. Numerical simulations of the performed test are carried out using the explicit solver of the finite element software package LS-Dyna R9.0.1. The model used in the simulation implemented through the user material subroutine accounts for a yield function with a non-associated flow rule, a Swift–Voce strain hardening law and Johnson–Cook type of multipliers with the effects of strain rate and temperature. The stress-triaxiality, Lode angle parameter and strain-rate dependent Hosford–Coulomb fracture initiation model is employed to predict a steel failure, [3-4].

***KEYWORDS:** impact modelling, ductile fracture, armour steel, Lode angle parameter, stress triaxiality

1 Introduction

As the projectiles tip imposes a particular stress state in impacted targets, impact tests with projectiles with different shapes are often conducted to analyze the failure modes and the ballistic limit curves. Additionally, such tests may be used to validate plasticity and fracture models.

The study discusses a numerical modelling of impacts with projectiles of different tips with use of an user defined material model, where the function describing the material is a quadratic plasticity model with a non-associated Hill'48 flow rule which couples a Johnson–Cook type of rate- and temperature dependency with a combined Swift–Voce strain hardening law. The model treats the temperature as an internal variable and thereby accounts for the effect of thermal softening in an approximate manner without solving the thermal field equations. Recent research on ductile fracture has demonstrated the importance of the effect of the Lode angle parameter [5–6]. For example, conventional fracture models cannot explain the drop in ductility for biaxial tension stress states ($0.33 < \eta < 0.667$), while Lode angle dependent theories, such as the Mohr–Coulomb and Hosford–Coulomb fracture initiation models can fully explain this phenomenon.

Armour steels are a family of steel grades specially designed for ballistic protection. They are characterized by high strength, hardness and moderate ductility – properties required to improve protective performance against ballistic and explosive threats. An armour steel known under the trade name Mars[®] 300, an ultrahigh hard armour (UHHA) martensitic steel designed for ballistic protection is the tested material. Mars[®] 300 steel is available as rolled homogenous plates with different thicknesses and also as plates with a regular circular hole pattern, so-called perforated plates, [7-8].

Parameters of the above introduced plasticity and fracture model are identified on the basis of material characterization tests and validated by modelling of impact tests in Mars[®] 300 perforated plates, [9].

2 Impact experiment

The impact experiments are conducted using a high-pressure single-stage gas gun, Fig. 1. The impact velocity is measured by a double-laser light barrier located near the exit of the gun muzzle. Impacts are also registered by a Shimadzu HPV1 high-speed camera, due to which the projectiles trajectory before and after plate perforation is followed, [1,9].

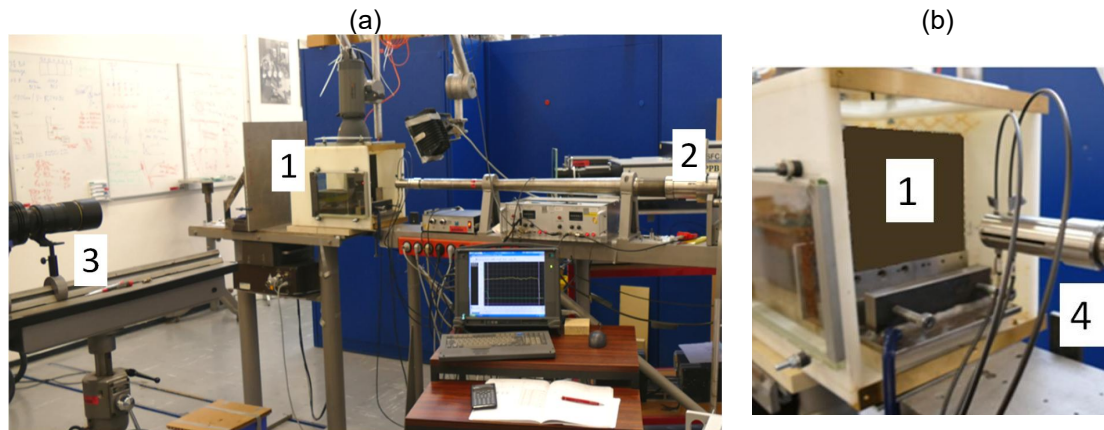


Fig. 1: Experimental set-up for the impact tests: [1] specimen mounted in a catch box, [2] single-stage gas gun, [3] high-speed camera for the side view, [4] gun barrel with a double-laser light barrier.

Projectiles with blunt, hemispherical and conical noses were cut by wire EDM from the steel plates with the initial thickness of 12 mm. Projectiles have the same mass of 13.8 g and diameter of 8 mm which results in different lengths; i.e. 39.6 mm, 36.3 mm and 35 mm for the conical, hemispherical and blunt striker, Fig. 2. A possible range of impact velocity for the given mass of strikers is 240 – 380 m/s.



Fig. 2: Strikers with different nose shapes used in the test.

Thinnest Mars[®] 300 plates available on the market have a thickness of 6mm. To ensure that strikers at the given mass and maximum possible velocity perforated plates, the initial plate thickness is reduced to 3 mm by grinding from only one side under permanent cooling to prevent any changes of the microstructure.

When thin ductile targets are impacted by projectiles which remain rigid after plate perforation, the final plate failure modes are strongly affected by the projectile tip geometries and they differ much depending on the tip shape. In the discussed examples, it may be observed that the plates fail due to plugging and the blunt projectiles at the highest possible impact velocity do not cause plate perforation, Fig.3. Petals, typically observed for perforated ductile plates, are not formed. The ductility of the armour steel materials is too low to favour their development. Hemispherical and conical strikers ejected plugs and some smaller debris in a shape of a ring with thickness of approximately 1.5 mm and diameter of ca. 7.7– 8 mm. It is observed that the exit holes, remained after the passage of the

conical impactors, are more irregular with sharp edges. The hemi-spherical impactor left in the target plate almost perfectly circular hole. The holes of approximately circular shapes through which passed the impactors are slightly larger than the projectiles' diameter (8.3 – 8.8 mm). Blunt projectiles caused regular, localized bulges of the diameter close to the diameter of the impactors. Their heights increased with the impact velocity and measured from the outer surface of the rear plate side vary between 2 – 4 mm. The blunt projectiles caused also the largest plate bending.

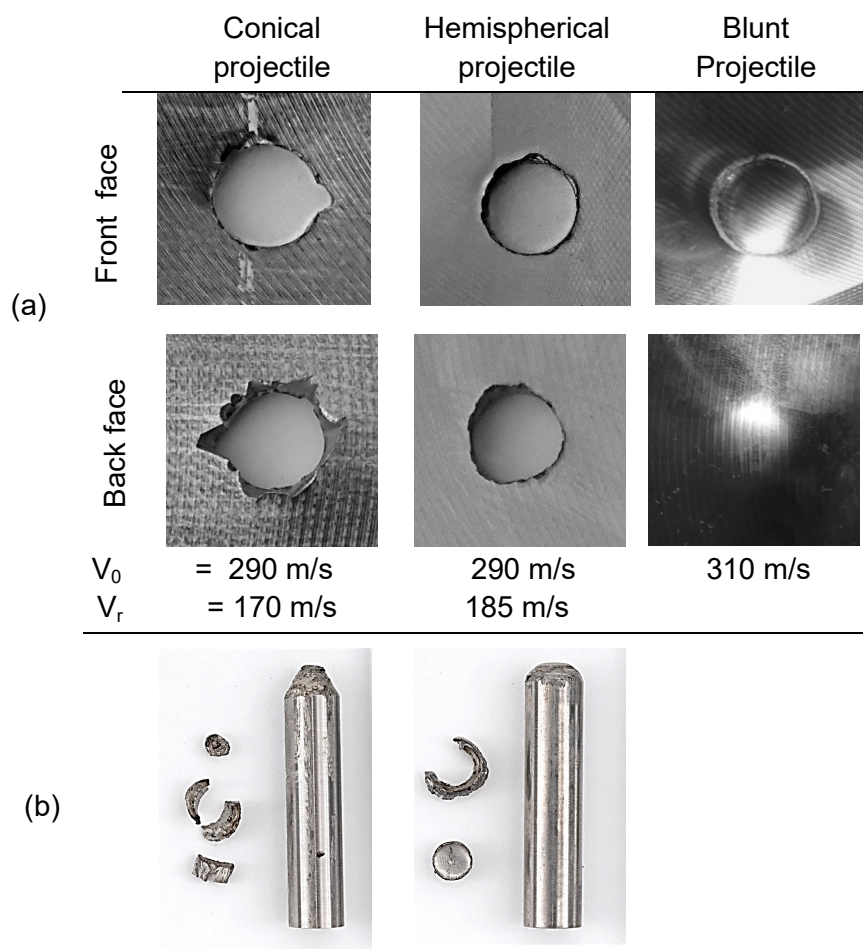


Fig.3: Perforation of 3 mm thick armour plates by different strikers: (a) targets and (b) projectiles.

The target material is sufficiently hard to induce a large plastic deformation into the projectile. Initially pointed nose of the conical projectiles is reduced which affects the size of plugs. The noses of hemispherical projectiles are deforming much less, so the shape of plugs is similar at all impact velocity with the diameter close to 4.6 mm, [1]. Due to the impacts at the velocity 290 m/s, the projectiles lengths are reduced to 35.86 mm and to 36.01 for the hemispherical and conical tips. The blunt projectiles became 3.4 mm shorter.

3 Numerical Simulations

Assuming the symmetry of the modelled configuration, only its quarter has been implemented into the calculation. Both the 3 mm thick target plate and the projectiles are meshed with reduced integration 8-node solid elements with stiffness-based hourglass control. The impact zone and the tip of the projectile are discretized with a fine mesh of element edge length 0.1 mm. The validation of the plasticity and fracture models was performed basing on the simulation of uniaxial tests of samples meshed by elements with this edge size, [11].

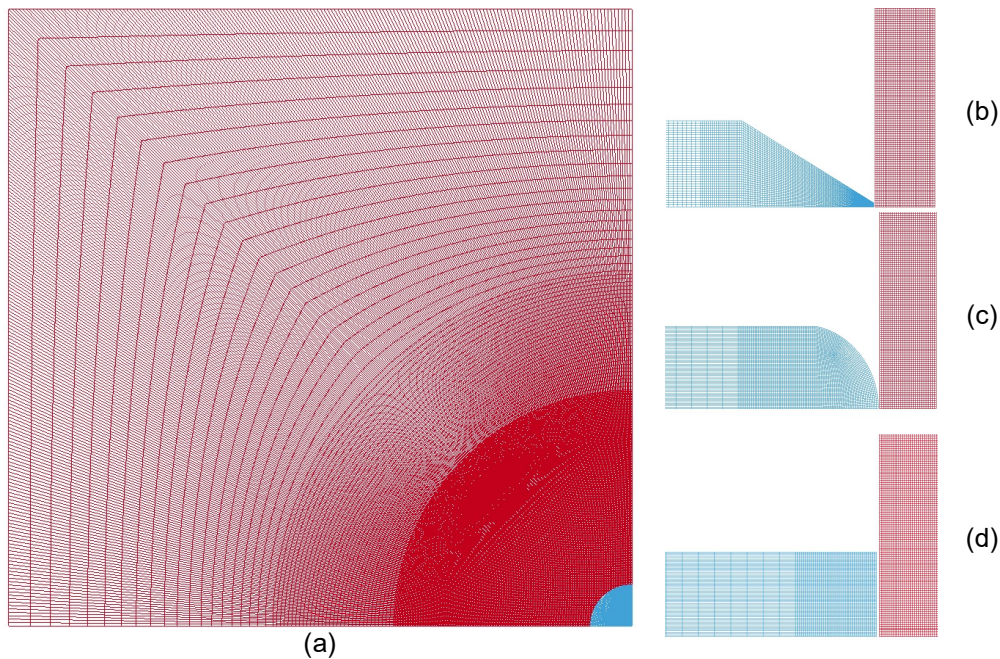


Fig.4: Mesh of the numerical configuration: a) top view and cross-section of the impact zone with the projectiles of b) conical, c) hemispherical and d) blunt nose.

In the target plate, this refined zone has the diameter of 20 mm and 30 elements through the plate thickness. The next zone of length 12 mm consists of elements with edge length 0.4 mm and finally, on the plate edges there are the widest elements with the edge length of 2 mm, Fig. 4. In total, the quarter of the target plate is meshed by 1.5 million of elements. The front part of the impactors is also meshed with 0.1 x 0.1 x 0.1 mm elements; the part not affected by the contact with the target plate is meshed by elements with length 1 mm – which results in almost 300000 elements for each projectile. To the plate, besides symmetry conditions, the boundary conditions are applied and it is clamped on its top and bottom edges. The impact velocity is imposed on the striker as the initial condition. A frictionless contact is chosen between the plate and the projectile with the contact option *ERODING_SURFACE_TO_SURFACE, which allows an element erosion.

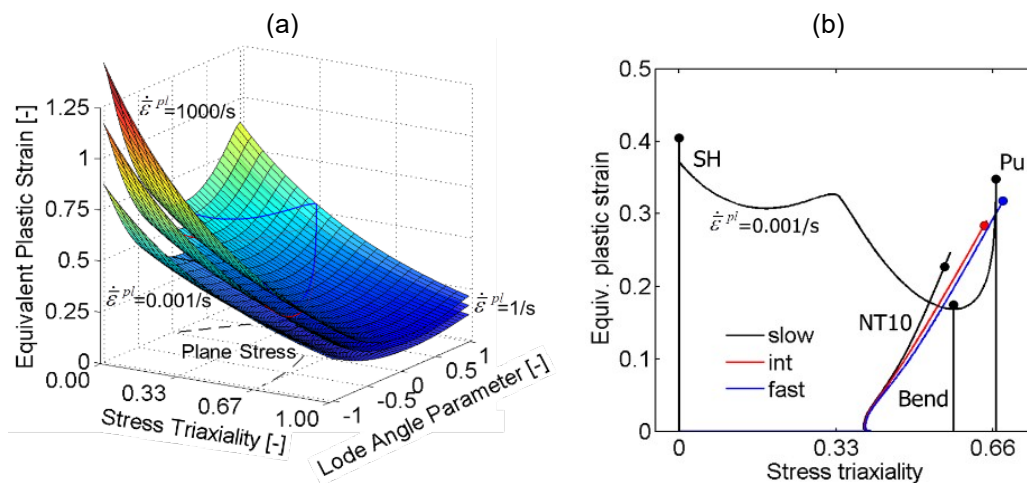


Fig.5: Fracture response of the Mars[®]300 steel: a) illustration of the fracture surfaces for different strain rates in the space of stress triaxiality, Lode angle parameter and equivalent plastic strain, b) the fracture envelope corresponding to the strain rate 0.001 s⁻¹.

The basic testing program for calibrating the material model included five different types of specimen geometries. In all experiments, the strain fields on the specimen surfaces are monitored using Digital Image Correlation. The equivalent strains reached about 0.4, 0.18 and 0.35 in the shear, plane strain

tension and equi-biaxial tension experiments, respectively. The strain and stress fields inside the specimens are identified through a hybrid-experimental-numerical approach, which involves the numerical modelling of all experiments. The parameters of the model required to perform calculations are given in Table 1, [9].

Figure 5a illustrates the effect of the strain rate on the resulting fracture surface for Mars[®] 300 in the space of equivalent plastic strain, stress triaxiality and Lode angle parameter. The loading path to fracture describing the evolution of the equivalent plastic strain at the strain rate 0.001 s^{-1} in terms of the stress triaxiality is shown in Fig. 5b.

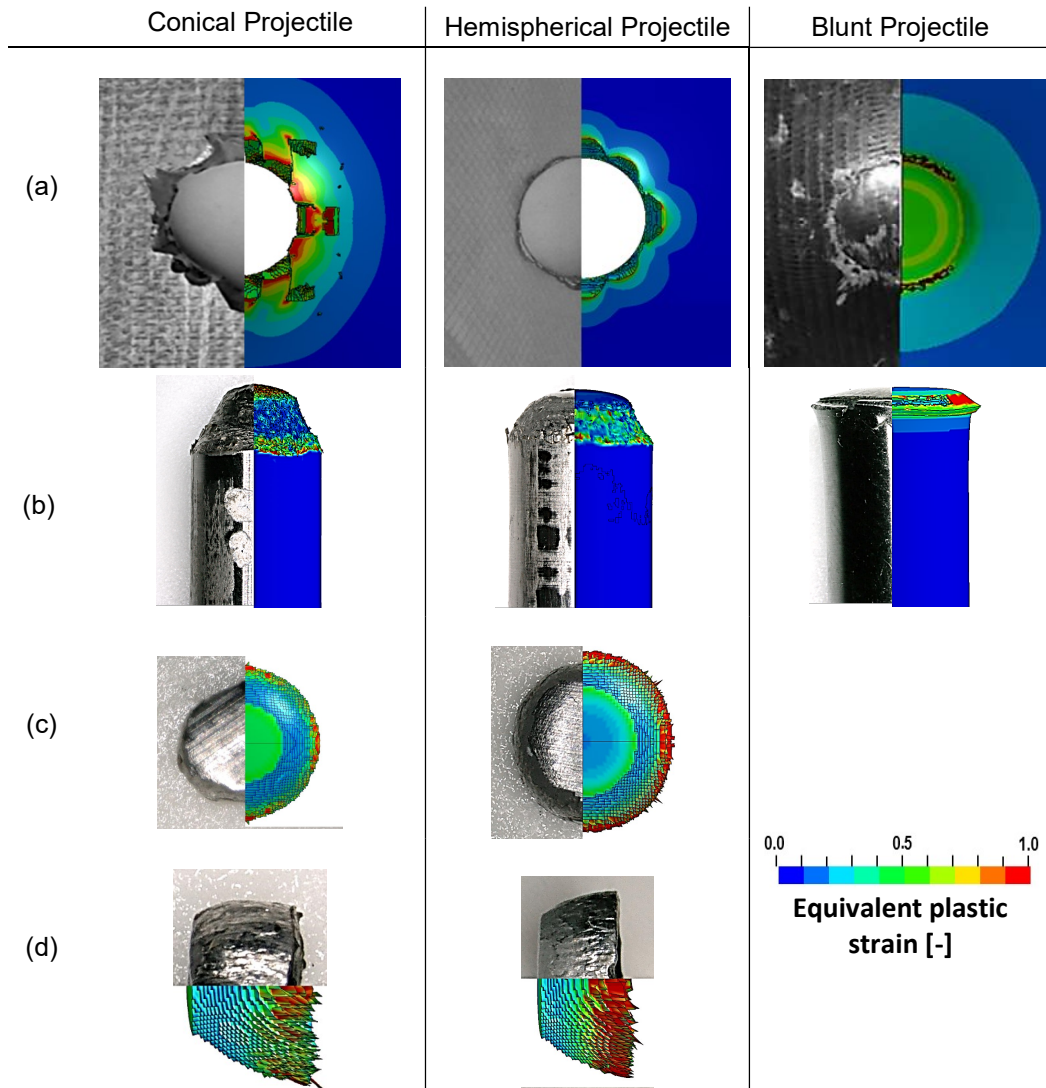


Fig. 6: Comparison of geometrical characteristics of: (a) exit holes (entry holes in the case of the blunt striker), (b) projectiles and (c) plugs remained after passage of impactors at impact velocity 290 m/s.

The numerical simulation was performed in the explicit solver of the finite-element code Ls-Dyna, in which the plasticity and fracture models were implemented by the UMAT subroutine but the model could also be used through *MAT_260B in the Ls-Dyna package. Application of this material model does not required an equation of state, additional add-erosion criterions are also redundant.

A [MPa]	ε_0 [-]	n [-]	k_0 [MPa]	Q [MPa]	β [-]
4439.57	0.000513	0.184	1318.14	1048.44	86.48
α [-]	$\dot{\varepsilon}_0$ [1/s]	C [-]	m [-]	T_{ref} [°C]	T_m [°C]
0.124	0.001	0.00188	1.394	25	1287
$\dot{\varepsilon}_{ad}$ [1/s]	C_p [kJ/kgK]	G_{12} [-]	G_{22} [-]	G_{44} [-]	
9.185	0.449	-0.472	0.985	2.99	
a [-]	b [-]	c [-]	γ [-]	n [-]	HC fracture initiation model
1.349	0.3254	0.0755	0.0494	0.1	

Table 1: The parameters of the used flow and fracture models.

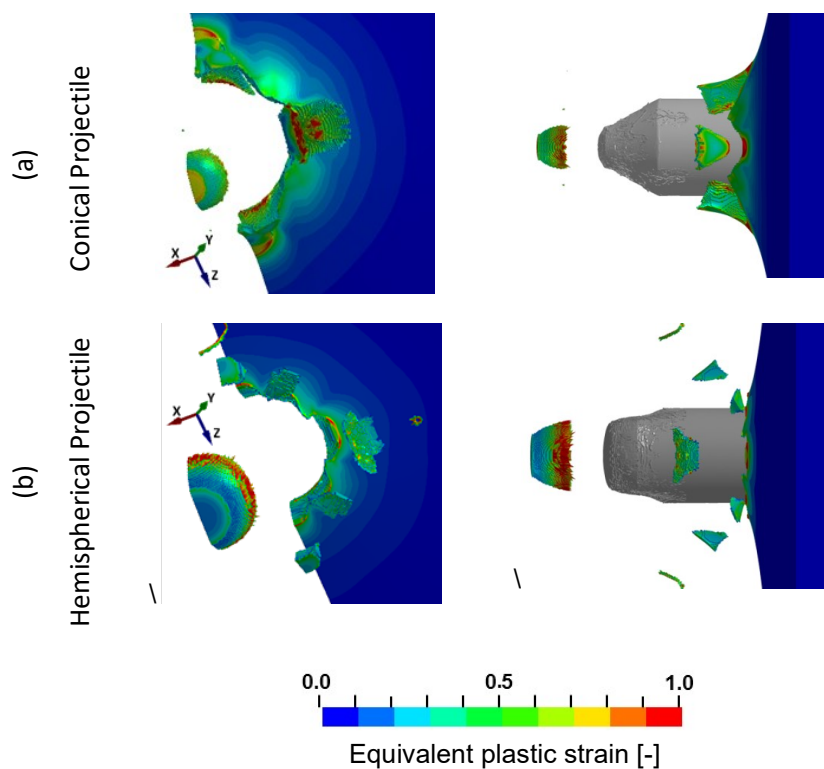


Fig. 7: Plate perforation by (a) conical and (b) hemispherical projectiles at 290 m/s.

Figure 6 shows the results of modelling by use of the aforementioned plasticity model and the fracture model which accounts for the triaxiality, Lode angle parameter and the strain rate. A good agreement of experiments and numerical simulations regarding both the shape of the targets and projectiles after the impacts. In all cases, the numerical simulation captures the geometrical features of the tests' components. As in the experiment, the blunt striker does not perforate the plate – a trace it left on the front plate face, as well its deformation are well represented in the simulation. The exit of the hemispherical projectile is smoother than the exit hole remained after the passage of the conical striker. The plastic deformation and the erosion of the tips of all three projectiles are represented

accurately in the simulation. The shape of the conical impactor has been eroded, so as it resembles the shape of the hemispherical projectile. The numerical simulations also predict the formation of plugs which shapes are similar to those observed experimentally. They are less compressed – 2.6 mm comparing to 2.4 mm measured in the experiment. Both in the experiment and in the simulation, the plugs are wider at their basis (which was in direct contact with the projectile), having the diameter close to that of the projectile at the moment of the impact. Debris of smaller size is ejected from the plates in the simulations (Fig. 7) but they do not have a specific ring-shape observed experimentally as they are fragmented. The projectile velocity according to the simulation drops to 165 m/s and to 155 m/s for the hemispherical and the conical striker.

The simulation shows that the target deformation changes according to the striker geometry, even if differences dependent on the nose shape are not as distinct as it is observed due to perforation of less hard metal plates by rigid strikers.

4 Conclusions

The presented study describes a numerical modelling of the impact test, in which projectiles with different nose shapes at velocity close to 300 m/s strike 3 mm thick plates manufactured from a high strength and high hardness armour steel. The Mars[®] 300 steel is modelled by use of a quadratic yield function with non-associated flow rule, a modified Swift–Voce strain accounted for strain rate and temperature. To predict the onset of a crack, the Hosford–Coulomb fracture model is used.

The results are in good agreement with the experimental observations modelling correctly the modes of perforation observed experimentally. The failure mechanisms are similar in the case of the hemispherical and conical striker. Due to the contact with the hard steel, the conical projectile deforms and loses its pointed tip becoming similar to a projectile with a hemispherical tip. The targets do not show failure modes other than plugging and the blunt striker at the given velocity do not have sufficient energy to cause plate perforation.

The applied material model accounts for the effects of strain rate, temperature, stress triaxiality and Lode parameter, which provides good predictive capabilities and allows an insight into the deformation and failure mechanisms of both projectiles and targets extracted from an armour steel.

References

- [1] Fras T, Roth CC and Mohr D. Dynamic Perforation of Ultra-hard High-Strength Armour Steel: Impact Experiments and Modelling submitted to Int J Impact Eng.
- [2] Industeel Brochure. MARS[®] 300 perforated MARS[®]300. France: Industeel; 2015 November.
- [3] Dunand M and Mohr D. Effect of Lode parameter on plastic flow localization after proportional loading at low stress triaxialities. J Mech Physics Solids 2014; 66: 133-53.
- [4] Mohr D and Marcadet JC. Micromechanically-motivated Phenomenological Hosford-Coulomb Model for Predicting Ductile Fracture Initiation at Low Stress Triaxialities, Int J Solids Structures 2015; 67-68: 40-55.
- [5] Roth CC and Mohr D. Effect of Strain Rate on Ductile Fracture Initiation in Advanced High Strength Steel Sheets: Experiments and Modelling. Int J Plasticity 2014; 56: 19–44.
- [6] Roth CC and Mohr D. Ductile fracture experiments with locally proportional loading histories. Int J Plasticity 2016; 79:328-54.
- [7] Fras T, Murzyn A and Pawlowski P. Defeat mechanisms provided by slotted add-on bainitic plates against small-calibre 7.62 mm x 51 AP projectiles. Int J Impact Eng 2017; 103:241-53.
- [8] Fras T, Faderl N. Influence of add-on perforated plates on the protective performance of light-weight armour systems. Problems of Mechatronics. Armament, Aviation, Safety Engineering 2018;9.1(131):31-48.
- [9] Fras T, Roth CC and Mohr D. Fracture of high-strength armour steel under impact loading. Int J ImpactEng 2018; 111: 147-64.